Photogrammetric control of oblique Apollo Metric Camera images

Kenneth L. Edmundson[1],Oleg Alexandrov[2], Brent A. Archinal[1], Kris J. Becker[1], Tammy L. Becker[1], Zachary M. Moratto[2], Ara V. Nefian[2], Janet O. Richie[1], Mark S. Robinson[3]

1–Astrogeology Science Center, U.S. Geological Survey, Flagstaff, AZ 86001, USA; 2–NASA Ames Research Center, Moffett Field, CA 94035, USA; 3–School of Earth and Space Exploration, Arizona State University, Tempe, AZ 85287, USA

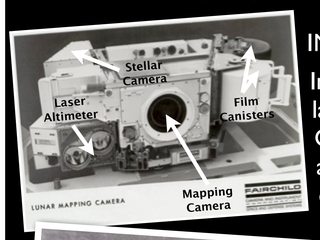

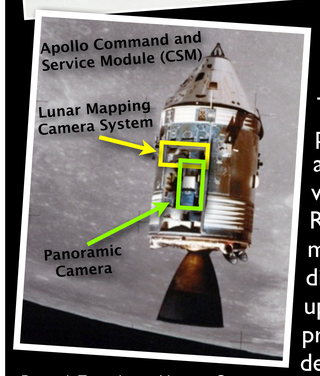

Figure 1. Top - Lunar Mapping Camera system (NASA/Fairchild). Bottom - Apollo Command and Service Module (CSM) with Lunar Mapping Camera system and Panoramic camera in the Scientific Instrumentation Module (From NASA image AS15-88-11972).

INTRODUCTION

In the early 1970s, an integrated photogrammetric mapping system (Figure 1) flew on the last three Apollo lunar missions (15, 16, and 17). Included was a Metric (mapping) Camera (MC), a high-resolution Panoramic Camera (PC), and a star camera and laser altimeter to provide support data [1]. Approximately 6,000 MC images of the lunar equatorial region were acquired that are suitable for mapping. Of these, ~3/4 are nadir-pointed, covering ~16% of the lunar surface. The remaining ~1,500 images are oblique, increasing useful coverage to ~25%.

The NASA Johnson Space Center (JSC) and Arizona State University (ASU) recently produced digital scans of the original MC negatives at film-grain resolution and created an digital record of support data (available online at http://apollo.sese.asu.edu) [2,3]. This work enables an ongoing collaboration between USGS Astrogeology, the Intelligent Robotics Group of the NASA Ames Research Center (ARC), and ASU to achieve the most complete cartographic development of Apollo mapping system data into versatile digital map products. These can be integrated easily with other digital lunar data and updated geodetically and cartographically as needed. Scientific/engineering uses of these products including mission planning, geologic mapping, geophysical process modeling, slope dependent correction of spectral data, and change detection.

With the Ames Stereo Pipeline (ASP) [4] and the Integrated Software for Imagers and Spectrometers (ISIS) developed by the USGS [5], the ARC has completed our initial joint project to process the nadir images by making a photogrammetrically and geodetically controlled, orthorectified digital image mosaic (DIM) and digital terrain model (DTM) sampled at ~30 m/pixel and tied to a reference frame based on Lunar Orbiter Laser Altimeter (LOLA) data [6]. To complete processing of the MC images, we now focus on the oblique images, beginning with those from Apollo 15. The ~450 Apollo 15 oblique images were acquired in four orbits with the spacecraft oriented so the camera was tilted either 25° forward or aft; or 40° north or south (orbits 23, 34, 35, and 71). While oblique geometry may complicate feature recognition and orthorectification, the USGS has previously shown that such images can be rectified and provide valuable topographic information [7,8].

PHOTOGRAMMETRIC CONTROL OF OBLIQUE APOLLO 15 IMAGES

In the control process, images are registered to each other or the ground by measuring features common to overlapping images (tie points) or common between images and ground (control points). The Apollo images are pre-processed for quality and removal of artifacts (fiducials/reseaux; space hardware; image noise) that may complicate tie-point detection and the matching of tie-points between images. Image measurements are input to the least-squares bundle adjustment (jigsaw in ISIS [9]) which produces improved image position/attitude parameters and ground coordinates for all tie/control points. At this time, the oblique orbits have been controlled separately in ISIS (Table 1) using the Lunar Reconnaissance Orbiter Camera (LROC) Wide Angle Camera (WAC) mosaic [10] and LOLA DTM as ground control. With the improved image parameters we created preliminary DIMs (Figure 2) and updated (smithed) NAIF SPICE position/pointing kernels [11] for each orbit. Using these new kernels and the oblique images, the ARC produced a preliminary DEM for each orbit (Figures 3 and 4).

Table 1. Apollo 15 oblique orbit bundle adjustment statistics.

Orbit	# Images	# Points			RMS residuals (pixels)
		tie	control	measures	
23	115	907	12	3902	1.54
34	105	982	33	3350	1.51
35	116	727	6	2964	1.14
71	127	293	12	1428	1.12

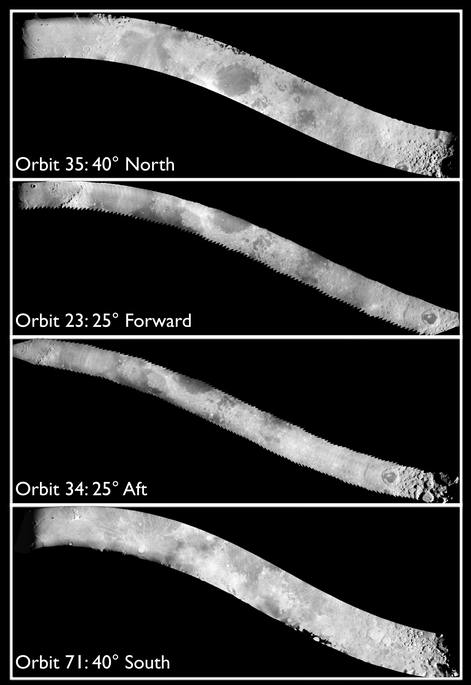

Figure 2. Preliminary controlled DIMs of Apollo 15 oblique orbits. Images are averaged. Projection is simple cylindrical. Original resolution 500 m/pixel.

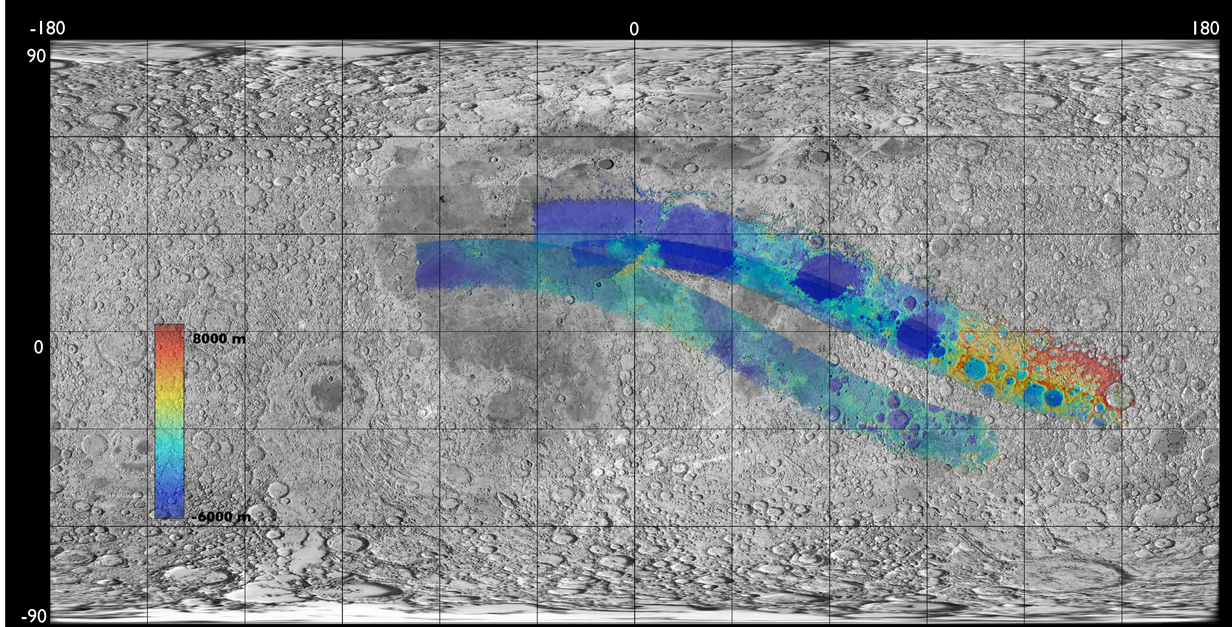

Figure 3. Individual, preliminary DTMs of Apollo 15 oblique orbits. Each orbit was controlled separately. Base layer is the airbrushed global lunar mosaic created by USGS. Elevations are approximate. Projection is simple cylindrical. Original resolution 500 m/pixel.

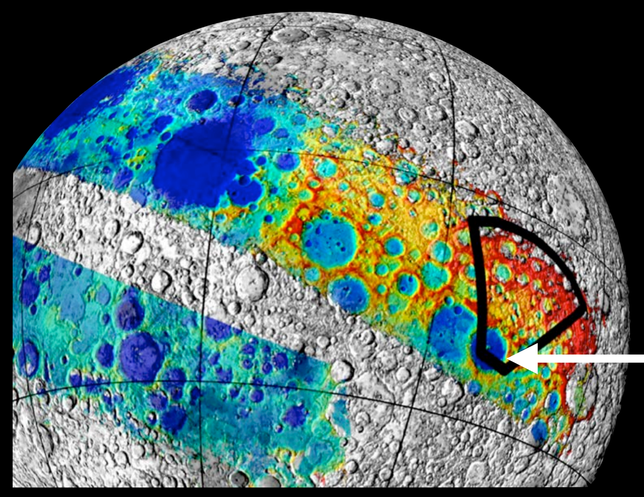

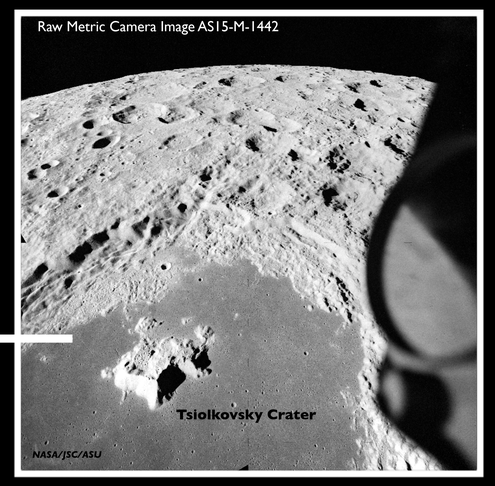

Figure 4. Left - Individual, preliminary DTMs of Figure 3 displayed on a sphere. The footprint is of image AS15-M-1442 (seen at right) from orbit #35 (40°N) which covers a portion of Tsiolkovsky Crater at the southern end.

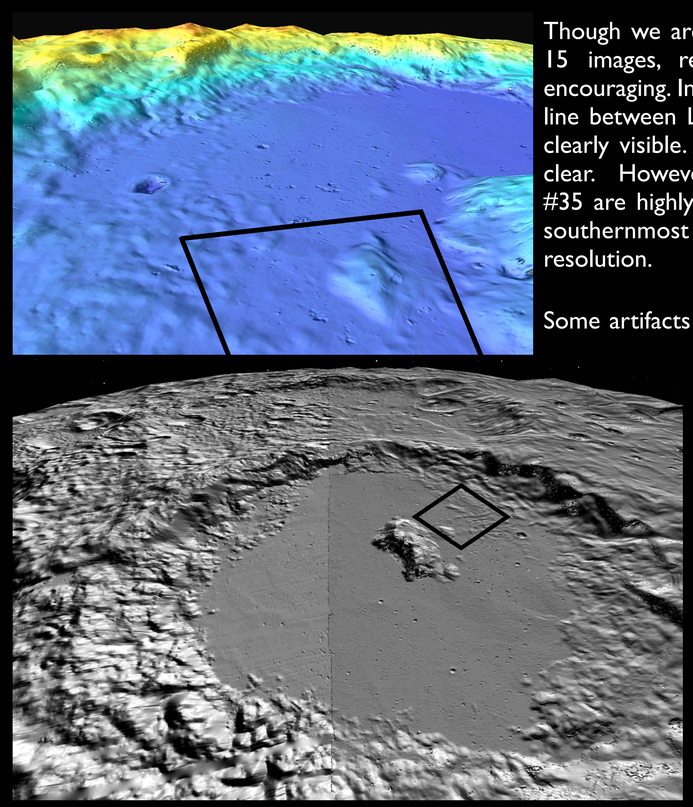

Figure 5. Zoomed, oblique views of Tsiolkovsky Crater. Top - Portion of orbit #35 DIM draped over orbit 35 DTM. View direction is approximately west. Bottom - Hillshaded view of combined LOLA (left) and Apollo orbit #35 (right) DTMs. View direction is approximately east. The black box in both images is the region of interest shown in Figure 6 below.

Though we are in the early stages of processing oblique Apollo 15 images, results to date, as shown in Figures 2-6 are encouraging. In the hillshaded oblique view in Figure 5 below, the line between LOLA (left) and Apollo orbit #35 (right) DTMs is clearly visible. A higher level of detail in the Apollo area is also clear. However, we should emphasize that the images of orbit #35 are highly oblique to the north and the area shown is the southernmost portion of this DTM and has the highest resolution.

Some artifacts are visible in the Apollo DTM in this area (Figure 6) and more appear as we look towards the limb in orbits #35 and #71. We are investigating the cause of these artifacts and hope to improve our process to eliminate or minimize their occurrence. We are also working to quantify the accuracy of the DTMs produced here.

ONGOING WORK

We are controlling the oblique and nadir Apollo 15 MC images to each other and to the LOLA reference frame. Tie-point extraction and image matching are nearly finished. After a complete control solution we will generate improved image position/pointing parameters. This will facilitate the creation of an updated DTM for the region. A new control solution will be performed with this DTM as ground control and improved position/pointing data will be regenerated. The process of performing control solutions and regenerating topography will be iterated as needed. Final products will include an expanded database of Apollo 15 MC tie-points (consistent with the LOLA reference frame); improved image position/pointing parameters in the form of NAIF SPICE kernels; and a DIM and DTM of the entire Apollo 15 region.

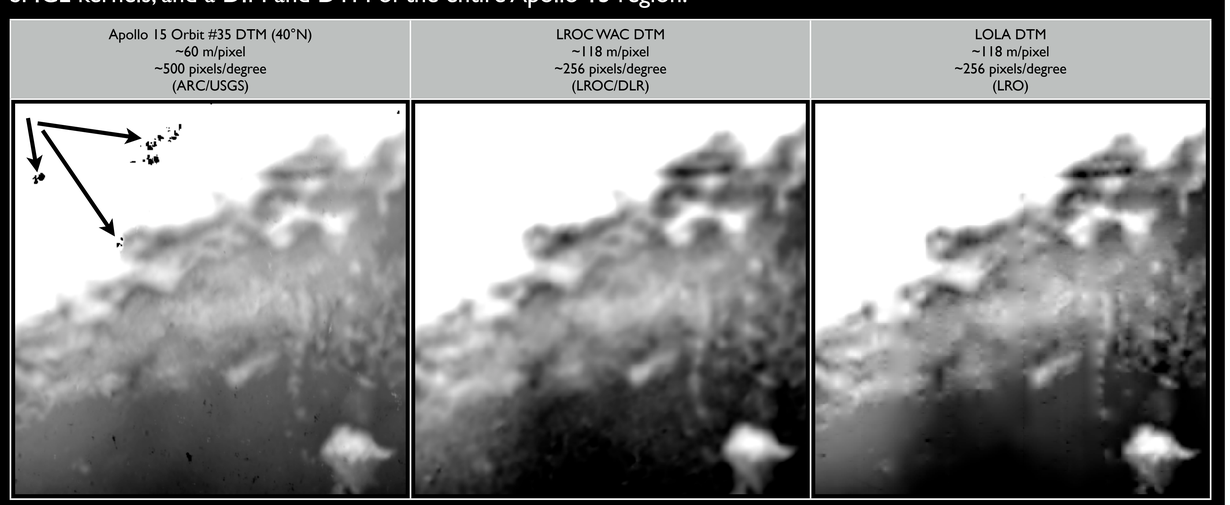

Figure 6. Visual comparison of DTMs within region of interest in Tsiolkovsky crater (Figure 5) shows a higher level of detail in the Apollo orbit #35 DTM. The most glaring artifacts visible in the Apollo DTM example here are indicated by black arrows.

REFERENCES

[1] Livingston, R.G., et al. (1980) Aerial Cameras, In Manual of Photogrammetry, 4th Ed., ASP, 187-278. [2] Robinson, M.S., et al. (2008) LPS XXXIX, Abstract #1515. [3] Paris, K.N., et al. (2012) LPS XLIII, Abstract #2273. [4] Moratto, Z., et al. (2010) LPS XLI, Abstract #2364. [5] Kestay, L., et al. (2014) LPS XLV, Abstract #1686. [6] Nefian, A., et al. (2012) LPS XLIII, Abstract #2184. [7] Wu, S.S.C., et al. (1972) In Apollo 16 Preliminary Sci. Report, NASA, SP-315, 30-5 to 30-10. [8] Gaddis, L.R., et al. (2005) Space Resources Roundtable VII: LEAG Conf. on Lunar Exploration, LPI 1287. [9] Edmundson, K.L., et al. (2012) ISPRS Annals, I-4, 203-208. [10] Henriksen, M.R., et al. (2013) LPS XLIV, Abstract #1676. [11] Acton, C.H., et al. (1996) Planet. Space Sci., 44(1), 65-70.

ACKNOWLEDGEMENTS

This work is funded by the NASA Lunar Advanced Science and Exploration Research program under contract #NNH12AU53I.